

# Light-front Nambu–Jona-Lasinio model at finite temperature and density

S. Strauß<sup>1</sup>, S. Mattiello<sup>2</sup>, and M. Beyer<sup>1</sup>

<sup>1</sup> Institute of Physics, University of Rostock, D-18051 Rostock, Germany

<sup>2</sup> Institut für Theoretische Physik, Universität Gießen, D-35392 Giessen, Germany

E-mail:

stefan.strauss@uni-rostock.de, stefano.mattiello@theo.physik.uni-giessen.de,  
michael.beyer@uni-rostock.de

**Abstract.** In recent years light-front quantisation has been extended to allow for a consistent treatment of systems at finite temperature and density. This is in particular interesting for an investigation of the processes in nuclear matter under extreme condition as occurring, e.g., during a heavy ion collision. Utilising a Dyson expansion to the  $N$ -point Green functions at finite temperature and density we focus on the occurrence of pionic and scalar diquark dynamics in quark matter and compute the masses and the Mott dissociation using a separable  $t$ -matrix approach. For the scalar quark-quark correlation we determine the critical temperature of colour superconductivity using the Thouless criterion. On the same footing the properties of the nucleon in a medium of quark matter are computed within a Faddeev approach. Critical lines for nucleon breakup are given. Presently, we use a light-front Nambu–Jona-Lasinio model that allows us to compare these results of this novel approach to the more traditional instant form approach, where applicable.

PACS numbers: 11.10.Wx, 12.38.Mh, 25.75.Nq

Submitted to: *J. Phys. G: Nucl. Phys.*

## 1. Introduction

Light-front quantisation recognized by Dirac [1] provides a framework to describe the perturbative and the nonperturbative regime of quantum chromodynamics (QCD), for an overview see e.g. [2]. The importance of light-front quantisation as a complement to Monte Carlo simulations has also recently been emphasized by Ken Wilson [3].

A description involving both regimes is necessary, if one is interested in the dynamics close to the chiral and the confinement-deconfinement transition that is suggested by lattice QCD [4, 5, 6, 7, 8], model analyses [9, 10, 11, 12], and through recent interpretations of certain RHIC results [13, 14, 15, 16, 17, 18, 19]. It seems that close to phase transition the quark gluon plasma does not appear as a weakly interacting gas of quarks and gluons but rather as a strongly correlated system. In the framework of many-body Green functions [20, 21], the inclusion of correlations can be achieved by the Dyson equation approach developed in the context of nonrelativistic nuclear physics, reviewed in [22]. This approach has been generalised to light-front quantisation to comply with the requirements of special relativity in [23], where also the necessary ingredients such as distribution functions, Green functions and Matsubara frequencies have been given. An early exploration of finite temperature QED(1+1) in discrete light cone quantisation has been done in Ref. [24] and the same theory has been reexamined in [25]. Further developments have been carried out and more examples given in Refs. [26, 27, 28, 29, 30, 31, 32, 33, 34, 35].

A formal framework of covariant calculations at finite temperatures in instant form has been given in Refs. [36, 37, 38] in a different context. Combination of the covariant statistical physics and light-front quantisation leads to the notion of general light-front coordinates first introduced in [30]. These coordinates allow the formulation of thermal field theory within the light-front frame and help to overcome the feature that the heat bath is moving with time-like velocity, while the time direction vector is light-like. Choosing a certain set of parameters the oblique frame in [30] reduces to the general light-front frame suggested in [23, 27] which correspond to a heat bath at rest in the instant form. The transformation is repeated here for completeness [30]

$$\begin{aligned} x^{\bar{0}} &= x^+, & x_{\bar{0}} &= x_0, & x_{\perp} &= (x_1, x_2), \\ x^{\bar{3}} &= x^3, & x_{\bar{3}} &= -2x_-, & x^{\perp} &= (x^1, x^2). \end{aligned} \quad (1)$$

One recognizes that in (1) light cone and instant form coordinates get mixed and the covariant time component is light cone time while the contravariant component is ordinary time. The metric can be derived by requiring invariance of the Minkowski line element and the important condition  $g_{\bar{0}\bar{0}} > 0$  holds. Therefore the medium velocity can be expressed as  $u^\mu = (1/\sqrt{g_{\bar{0}\bar{0}}}, 0, 0, 0)$  and fulfills  $u^2 = 1$ . Only few applications of thermal field theory in the general light cone frame are found in the literature.

Here we explore finite temperature and density properties of few-body, namely one-, two- and three-body systems in the Nambu–Jona-Lasinio (NJL) model that reproduces some low energy phenomenology of QCD, in particular its chiral properties, in a rather

transparent way, and yet includes spontaneous symmetry breaking as a nontrivial feature to be handled by light-front quantisation. The investigation of the one- and two-body sector confirms known results, like the phase boundary of chiral restoration, the pion Mott transition, the onset of two flavour colour superconductivity, from earlier calculations [39, 40] and exemplifies the equivalence of thermal field theory in the front and instant form. The three-body part consists of new results within this approach.

This paper is organized as follows. In the second Section we derive the explicit form of the meanfield thermal fermion propagator using general light cone coordinates and thereby showing that one recovers the propagator expected in the ordinary light-front frame. In Section 3 the propagator is embedded into the general framework of the Dyson expansion of many-body Green functions. A systematic treatment for two- and three-body correlations in the quark matter medium is developed. The last two Sections are concerned with applications of the framework to correlations of two and three light quarks in meanfield approximation. The Mott dissociation lines of the mesons and nucleons are computed and plotted in the phase diagram of quark matter.

## 2. Light-front equilibrium Green functions

Let us summarise aspects of thermal field theory in the light-front form and derive the free, in-medium Green function. In the generalised coordinates (1) the product  $u \cdot P$  is given by  $P_0/\sqrt{g_{00}}$  and the grand canonical partition function reads

$$Z_G = \text{Tr} \exp \{ -(P_0/\sqrt{g_{00}} - \mu N)/T \} = \text{Tr} \exp \{ -(P_+ + P_- - \mu N)/T \}, \quad (2)$$

where  $T$  is the scalar rest frame temperature and  $\mu$  the chemical potential belonging to the charge  $N$ . We introduce  $H_{\text{eff}} \equiv P_+ + P_- - \mu N$  and the statistical operator  $\rho_Z = e^{-H_{\text{eff}}/T}/Z_G$ . The four-momentum operator and the charge are

$$P^\mu = \int d^2x^\perp dx^3 T^{\bar{0}\mu}(x) = \int d^2x^\perp dx^3 T^{+\mu}(x), \quad (3)$$

$$N = \int d^2x^\perp dx^3 J^{\bar{0}}(x) = \int d^2x^\perp dx^3 J^+(x), \quad (4)$$

where  $T^{\mu\nu}(x)$  denotes the energy momentum tensor and  $J^\mu(x)$  the conserved current. Note that in (3) and (4) the light cone densities are integrated over three dimensional space and not the light-front plane.

The general light cone time-ordered (causal) Green function is

$$\mathcal{G}_{\alpha\beta}(x-y) = \theta(x^{\bar{0}} - y^{\bar{0}}) \mathcal{G}_{\alpha\beta}^>(x-y) + \theta(y^{\bar{0}} - x^{\bar{0}}) \mathcal{G}_{\alpha\beta}^<(x-y), \quad (5)$$

with the correlation functions

$$\mathcal{G}_{\alpha\beta}^>(x^{\bar{0}} - y^{\bar{0}}, \bar{x} - \bar{y}) = -i \langle \Psi_\alpha(x) \bar{\Psi}_\beta(y) \rangle, \quad (6)$$

$$\mathcal{G}_{\alpha\beta}^<(x^{\bar{0}} - y^{\bar{0}}, \bar{x} - \bar{y}) = \mp (-i) \langle \bar{\Psi}_\beta(y) \Psi_\alpha(x) \rangle, \quad (7)$$

and the notation  $\bar{x} = (x^{\bar{1}}, x^{\bar{2}}, x^{\bar{3}})$ . Here and in the following the upper (lower) sign is for fermions (bosons). The anti-causal Green function can be defined correspondingly. In

the generalised Heisenberg picture the light cone time dependence of operators is given by

$$\mathcal{O}(x^{\bar{0}}, \bar{x}) = e^{iH_{\text{eff}}x^{\bar{0}}} \mathcal{O}(0, \bar{x}) e^{-iH_{\text{eff}}x^{\bar{0}}}. \quad (8)$$

This differs from the regular Heisenberg picture of the vacuum by the thermodynamic constraints. In equilibrium the average is taken over the (equilibrium) grand canonical statistical operator  $\rho_G$ , viz.  $\langle \cdots \rangle = \text{tr}\{\rho_G \cdots\}$  and in addition  $\mathcal{G}_{\alpha\beta}^<$  and  $\mathcal{G}_{\alpha\beta}^>$  are related by (anti) periodic boundary conditions,

$$\mathcal{G}_{\alpha\beta}^<(x^{\bar{0}}, \bar{x}) = \pm \mathcal{G}_{\alpha\beta}^>(x^{\bar{0}} - i\beta, \bar{x}). \quad (9)$$

Therefore, in equilibrium, only one Green function needs to be considered, and, alternatively to (5), we may introduce the thermodynamic Green function [21]

$$\mathcal{G}_{\alpha\beta}^{\tau-\tau'} = -\langle T_{\tau} \Psi_{\alpha}(\tau) \bar{\Psi}_{\beta}(\tau') \rangle. \quad (10)$$

Setting  $x^+ = -i\tau$  (“imaginary time”) in (8) we achieve the thermodynamic Heisenberg picture. The Green functions (5) and (10) are related by their spectral representation utilising analytic continuation of the respective spectral functions just as in the instant form case [21]. To be more specific, in momentum space we introduce the spectral function  $A(k_{\bar{0}}, \underline{k})$

$$\mathcal{G}^<(k_{\bar{0}}, \underline{k}) = f(k_{\bar{0}}, \underline{k}) A(k_{\bar{0}}, \underline{k}) \quad (11)$$

$$\mathcal{G}^>(k_{\bar{0}}, \underline{k}) = (1 - f(k_{\bar{0}}, \underline{k})) A(k_{\bar{0}}, \underline{k}) \quad (12)$$

where  $A(k_{\bar{0}}, \underline{k}) = i(\mathcal{G}^>(k_{\bar{0}}, \underline{k}) - \mathcal{G}^<(k_{\bar{0}}, \underline{k}))$  and  $\underline{k}$  abbreviates  $(k_{\bar{1}}, k_{\bar{2}}, k_{\bar{3}})$ . Using (5) along with (11) and (12) the causal Green function can be represented as

$$\mathcal{G}(k_{\bar{0}}, \underline{k}) = \int_{-\infty}^{\infty} \frac{d\tilde{k}_{\bar{0}}}{2(2\pi)} \left[ \frac{f(\tilde{k}_{\bar{0}}, \underline{k}) A(\tilde{k}_{\bar{0}}, \underline{k})}{\frac{1}{2}k_{\bar{0}} - \frac{1}{2}\tilde{k}_{\bar{0}} - i\varepsilon} + \frac{(1 - f(\tilde{k}_{\bar{0}}, \underline{k})) A(\tilde{k}_{\bar{0}}, \underline{k})}{\frac{1}{2}k_{\bar{0}} - \frac{1}{2}\tilde{k}_{\bar{0}} + i\varepsilon} \right]. \quad (13)$$

A similar equation holds for (10), where the  $i\varepsilon$  term can be dropped

$$\mathcal{G}(k_{\bar{0}}^n, \underline{k}) = \int_{-\infty}^{\infty} \frac{d\tilde{k}_{\bar{0}}}{2(2\pi)} \frac{A(\tilde{k}_{\bar{0}}, \underline{k})}{\frac{1}{2}k_{\bar{0}}^n - \frac{1}{2}\tilde{k}_{\bar{0}}} \quad (14)$$

and the Matsubara frequencies are given by

$$\frac{1}{2}k_{\bar{0}}^n = \begin{cases} i(2n+1)\pi T + \mu & \text{fermions,} \\ i2n\pi T + \mu & \text{bosons.} \end{cases} \quad (15)$$

One may introduce traditional light cone coordinates via (1) into the equations (11) to (14), since they only depend on the difference  $k_{\bar{0}} - \tilde{k}_{\bar{0}}$ . Then the Matsubara frequencies in  $k^-$  read

$$\frac{1}{2}k_-^n = \begin{cases} i(2n+1)\pi T + \mu - \frac{1}{2}k^+ & \text{fermions,} \\ i2n\pi T + \mu - \frac{1}{2}k^+ & \text{bosons,} \end{cases} \quad (16)$$

and have been given before in Ref. [23] without the introduction of the general light-front frame. For an ideal gas (and also in Hartree-Fock approximation utilised later on) the spectral function is

$$\begin{aligned} A(k_{\bar{0}}, \underline{k}) &= 2\pi (\gamma k + m) \epsilon(k_{\bar{0}}) \delta(k^2 - m^2) \\ &= 2\pi \frac{\gamma k + m}{-2k_{\bar{3}}} \epsilon(k_{\bar{3}}) \delta(k_{\bar{0}} - k_{\bar{0}, \text{on}}), \end{aligned} \quad (17)$$

where  $\epsilon(x)$  denotes the sign function. Inserting (17) into (13) and transforming from general light cone frame back to the traditional one leads to

$$\mathcal{G}(k) = \frac{\gamma k_{\text{on}} + m}{k^+} \epsilon(k^+) \left( \frac{f(k^+, k_{\perp})}{k^- - k_{\text{on}}^- - i\varepsilon} + \frac{1 - f(k^+, k_{\perp})}{k^- - k_{\text{on}}^- + i\varepsilon} \right), \quad (18)$$

with  $k_{\text{on}}^- = (\vec{k}_{\perp}^2 + m^2)/k^+$ . Separating positive from negative  $k^+$  components and introducing the grand canonical Fermi distribution functions of particles  $f^+ \equiv f$  and antiparticles  $f^-(k^+) = 1 - f^+(-k^+)$

$$f^{\pm}(k^+, \vec{k}_{\perp}) = \left[ \exp \left\{ \frac{1}{T} \left( \frac{1}{2} k_{\text{on}}^- + \frac{1}{2} k^+ \mp \mu \right) \right\} + 1 \right]^{-1} \quad (19)$$

Eq. (18) changes to

$$\begin{aligned} \mathcal{G}(k) &= \frac{\gamma k_{\text{on}} + m}{k^- - k_{\text{on}}^- + i\varepsilon} \frac{\theta(k^+)}{k^+} (1 - f^+) + \frac{\gamma k_{\text{on}} + m}{k^- - k_{\text{on}}^- - i\varepsilon} \frac{\theta(k^+)}{k^+} f^+ \\ &\quad + \frac{\gamma k_{\text{on}} + m}{k^- - k_{\text{on}}^- + i\varepsilon} \frac{\theta(-k^+)}{k^+} f^- + \frac{\gamma k_{\text{on}} + m}{k^- - k_{\text{on}}^- - i\varepsilon} \frac{\theta(-k^+)}{k^+} (1 - f^-), \end{aligned} \quad (20)$$

which has been given before in Ref. [41] following naively a direct approach to light-front Green functions. However, the results are as shown equal and the particle propagator, that is setting  $f^- = 0$  in (20), can be found in Ref. [23]. In comparison to (20) the Green function given in Ref. [27, 32] were derived using the closed time path formalism and have therefore  $2 \times 2$  matrix structure. These Green function are suited to non-equilibrium situations, while we here concentrate on the equilibrium or close-to-equilibrium systems, which is why (20) is sufficient.

### 3. Dyson expansion

To investigate bound states in hot and dense quark matter we use techniques of the many-body Green functions organizing the equations into a Dyson expansion that leads to a hierarchy of linked cluster equations. This approach for the investigation of correlations in many-body systems at finite temperature and density was derived by P. Schuck and collaborators [22]. Furthermore this formalism was extended to the light-front in [23] to investigate three-quark correlations in quark matter. In the following we present a covariant derivation of the Dyson approach on the light-front and its application for mesonic and baryonic bound states. The Dyson approach to many-body Green functions in the light-front quantisation allows to calculate systematically the properties of few-body clusters, in particular of the two-quark bound states (viz.

pion) and of the three-quark clusters (viz. nucleon). This sets up the framework to investigate the change from nuclear to quark matter. One starts from the generalisation of the casual Green function given by

$$\begin{aligned} G_{\alpha\beta}^{x^{\bar{0}}-x'^{\bar{0}}} &= -i\langle T_{x^{\bar{0}}} A_\alpha(x^{\bar{0}}) A_\beta^\dagger(x'^{\bar{0}}) \rangle \\ &= -i\theta(x^{\bar{0}} - x'^{\bar{0}}) \langle A_\alpha(x^{\bar{0}}) A_\beta^\dagger(x'^{\bar{0}}) \rangle \pm i\theta(x'^{\bar{0}} - x^{\bar{0}}) \langle A_\beta^\dagger(x'^{\bar{0}}) A_\alpha(x^{\bar{0}}) \rangle. \end{aligned} \quad (21)$$

The operators  $A_\alpha(x^{\bar{0}})$  can be build out of any number of field operators (fermions and/or bosons) and their light cone time dependence in the Heisenberg picture follows Eq. (8). For the free fermion field, i.e.  $A(x^{\bar{0}}) = \Psi(x^{\bar{0}})$ , the standard light-front propagator (5) is recovered.

From the definition of the Green function at finite temperature we can derive the Dyson equation

$$i\partial_{\bar{0}} G_{\alpha\beta}^{x^{\bar{0}}-x'^{\bar{0}}} = \delta(x^{\bar{0}} - x'^{\bar{0}}) N_{\alpha\beta}^{x^{\bar{0}}} + R_{\alpha\beta}^{x^{\bar{0}}-x'^{\bar{0}}}, \quad (22)$$

where  $\partial_{\bar{0}}$  is the derivation with respect to  $x^{\bar{0}}$  and

$$N_{\alpha\beta}^{x^{\bar{0}}} = \langle [A_\alpha, A_\beta^\dagger]_\pm(x^{\bar{0}}) \rangle, \quad R_{\alpha\beta}^{x^{\bar{0}}-x'^{\bar{0}}} = -i\langle T_{x^{\bar{0}}} [A_\alpha, H](x^{\bar{0}}) A_\beta^\dagger(x'^{\bar{0}}) \rangle. \quad (23)$$

With the following definition of the mass matrix

$$M_{\alpha\beta'}^{x^{\bar{0}}-\bar{x}^{\bar{0}}} = \sum_{\alpha'} \int dx^{\bar{0}} R_{\alpha\alpha'}^{x^{\bar{0}}-x_1^{\bar{0}}} (G^{-1})_{\alpha'\beta'}^{x_1^{\bar{0}}-\bar{x}^{\bar{0}}} \quad (24)$$

the Dyson equation (22) can be written as

$$i\partial_{\bar{0}} G_{\alpha\beta}^{x^{\bar{0}}-x'^{\bar{0}}} = \delta(x^{\bar{0}} - x'^{\bar{0}}) N_{\alpha\beta}^{x^{\bar{0}}} + \sum_{\beta'} \int d\bar{x}^{\bar{0}} M_{\alpha\beta'}^{x^{\bar{0}}-\bar{x}^{\bar{0}}} G_{\beta'\beta}^{\bar{x}^{\bar{0}}-x'^{\bar{0}}}. \quad (25)$$

The mass matrix describes the modification of the particles energy and of the interaction due to the medium. The expression (24) for the mass operator is not well suited for practical computations. However, after some formal manipulations, the mass operator reads

$$\begin{aligned} M_{\alpha\beta'}^{x^{\bar{0}}-\bar{x}^{\bar{0}}} &= \sum_{\alpha'} [\delta(x^{\bar{0}} - \bar{x}^{\bar{0}}) \langle [[A_\alpha, H], A_{\alpha'}^\dagger]_\pm(x^+) \rangle \\ &\quad - i\langle T_x^{\bar{0}} [A_\alpha, H](x^+) [H, A_{\alpha'}^\dagger](x_1^{\bar{0}}) \rangle_{\text{irr.}}] (N^{-1})_{\alpha'\beta'}^{x^{\bar{0}}}. \end{aligned} \quad (26)$$

This equation separates the mass matrix in a instantaneous term  $M_{0,\alpha\beta'}$  related to the meanfield approximation and in a retardation (or memory) term  $M_{r,\alpha\beta'}^{x^{\bar{0}}-\bar{x}^{\bar{0}}}$ , i.e.

$$M_{\alpha\beta'}^{x^{\bar{0}}-\bar{x}^{\bar{0}}} = \delta(x^{\bar{0}} - \bar{x}^{\bar{0}}) M_{0,\alpha\beta'} + M_{r,\alpha\beta'}^{x^{\bar{0}}-\bar{x}^{\bar{0}}}. \quad (27)$$

Here, we neglect the retarded part of the mass operator which leads to the following equation of motion

$$\left( i\partial_{x^{\bar{0}}} - M_0^{x^{\bar{0}}} \right) G^{x^{\bar{0}}-x'^{\bar{0}}} = \delta(x^{\bar{0}} - x'^{\bar{0}}) N^{x^{\bar{0}}}, \quad (28)$$

where the indices  $\alpha, \beta$  are suppressed for simplicity.

For an explicit calculation of the expression for  $M_0$  and the normalisation factor  $N$  assumptions about the medium are needed. Here, we assume homogeneous matter

of non-interacting quarks and antiquarks. In this quasi-particle approximation the calculation of the mass operator and of the normalisation factor is performed in momentum space by introducing creations operators for the particles  $b^\dagger(\bar{k}, s)$  and antiparticles  $d^\dagger(\bar{k}, s)$ . The assumptions imply directly the Fermi distribution functions  $f^\pm(\bar{k})$ . For the one-body case one obtains the in-medium propagator (38) from the Dyson expansion. To investigate mesonic bound states we have to calculate the normalisation factor of the quark-antiquark system using (23). It reads

$$N_2(k_1, k_2) = 1 - f_1^+(k_1) - f_2^-(k_2) \quad (29)$$

and corresponds to the well-known Pauli blocking factor. Besides mesons three-quark bound states like the nucleon are subject of this paper, where we neglect the antiparticles degree of freedom. This is justified in light-front dynamics because pair creation processes are likely to be suppressed. The normalisation factor of the two-quark system is given by

$$N_2(k_1, k_2) = 1 - f_1 - f_2, \quad (30)$$

where  $f_i = f_i^+(k_i)$  for simplicity. The corresponding factor of the three-quark system is

$$N_3(k_1, k_2, k_3) = \bar{f}_1 \bar{f}_2 \bar{f}_3 - f_1 f_2 f_3, \quad (31)$$

where we used the notation  $\bar{f}_i = 1 - f_i$ . In general, the mass operator  $M_0$  can be separated into two terms: the first term,  $H_0$ , contains the self energy corrections in the effective mass and the second term describes the in-medium modified interaction. In the  $t$ -matrix equation we neglect the self energy term and consider in the following the term  $H_0$  only.

The resolvent operator  $R_0^{(n)}$  can be defined by

$$R_0^{(n)}(z) = \frac{1}{z - H_0}, \quad z \notin \sigma(H_0), \quad (32)$$

where  $n = 2, 3$  indicates the two- and three-quark correlations respectively. Hence the Dyson equation (28) yields

$$G_0^{(n)}(z) = R_0^{(n)}(z) N_n, \quad (33)$$

In this way the dominant medium effects due to Pauli blocking and self energy corrections are systematically included in the relativistic equations for the bound states, because the  $t$ -matrix equations contain  $G_0^{(n)}$  explicitly. In the case  $n = 2$  the resulting equation for the two-body  $t$ -matrix has the same formal structure as the Feynman-Galitzkii equation

$$T_2 = K + K R_0^{(2)} N_2 T_2 \quad (34)$$

where  $K$  represents the two-body interaction kernel. For  $n = 3$  the starting point is also given by the Bethe-Salpeter equation

$$T_3 = K + K R_0^{(3)} N_3 T_3. \quad (35)$$

A derivation of relativistic three-body equation on the light-front is formally identical to the nonrelativistic [42, 43] case, if we neglecting antiparticle degrees of freedom. Following [42, 43, 44] the resulting equation for the vertex function  $|\Gamma_\alpha\rangle$  reads

$$|\Gamma_\alpha\rangle = \sum_{\beta=1}^3 (1 - \delta_{\alpha\beta}) N_2^\beta T_2^\beta R_{2,\beta}^{(0)} |\Gamma_\beta\rangle, \quad (36)$$

where  $N_2^\beta$ ,  $T_2^\beta$  and  $R_{2,\beta}^{(0)}$  indicate the Pauli blocking factor, two-body  $t$ -matrix and the two-body resolvent in the channel  $\beta$ .

#### 4. NJL model at finite temperature and density on the light-front

In this Section we apply the light-front finite temperature field theory to the two flavour NJL model

$$\mathcal{L} = \bar{\psi}(i\gamma_\mu\partial^\mu - m_0)\psi + G((\bar{\psi}\psi)^2 + (\bar{\psi}i\gamma_5\boldsymbol{\tau}\psi)^2), \quad (37)$$

where  $\boldsymbol{\tau}$  are the Pauli matrices. In the meanfield approximation the chiral quark condensate contributes to the dynamical generated mass  $m = m_0 - 2g\langle\bar{\psi}\psi\rangle$ . Using (20) to compute the chiral quark condensate leads to the in-medium gap equation

$$m(T, \mu) = m_0 + 24G \int \frac{dk^+ d^2\vec{k}_\perp}{k^+(2\pi)^3} m(1 - f^+(k^+, \vec{k}_\perp) - f^-(k^+, \vec{k}_\perp)). \quad (38)$$

The medium independent first summand in the integral in (38) needs to be regularised, as usual the temperature modifications to the mass  $m(T, \mu)$  are finite. We like to use a consistent regularisation scheme for the gap equation and the related two-body calculations. Therefore the two-body bound state problem shall be discussed before treating the issue of regularisation of (38). The dependence of the constituent quark mass on the medium has been calculated within the NJL model on the light-front in Ref. [41].

##### 4.1. Pions

The pion  $t$ -matrix  $T_\pi(k)$  is obtained by the equation (34) that represented in momentum space reads

$$T_\pi(k) = K + \int \frac{d^4q}{(2\pi)^4} K G(q + k/2) G(q - k/2) T_\pi(k), \quad (39)$$

where  $K$  is some irreducible interaction kernel and  $G(q)$  the quark propagator taking into account the thermal mass (38). To arrive at (39) we replaced the two-body Green function  $G_0^{(2)}(q)$  by  $G(q - k/2)G(q + k/2)$  consistent with (33).

The separable interaction kernel in the pseudo-scalar channel reads

$$K_{\alpha\beta,\gamma\delta} = -2iG(\gamma_5\tau_i)_{\alpha\beta}(\gamma_5\tau_i)_{\gamma\delta}. \quad (40)$$



Introducing a reduced  $t$ -matrix  $t_\pi(k)$  via  $T_\pi(k)_{\alpha\beta\gamma\delta} = (\gamma_5\tau_j)_{\alpha\beta}t_\pi(k)(\gamma_5\tau_j)_{\gamma\delta}$  the solution to (39) is

$$t_\pi(k) = \frac{-2iG_\pi}{1 + 2G_\pi\Pi_\pi(k^2)}, \quad (41)$$

where  $\Pi_\pi(k^2)$  denotes the contribution of the bubble diagram for the pion. Evaluation of  $\Pi_\pi(k^2)$  using (33) (or equivalently (20)) leads to

$$\Pi_\pi(k^2) = -6 \int \frac{dx d^2\vec{q}_\perp}{x(1-x)(2\pi)^3} \frac{M_{2|0}^2(x, \vec{q}_\perp) (1 - f^+(M_{2|0}) - f^-(M_{2|0}))}{M_{2|0}^2(x, \vec{q}_\perp) - k^2}, \quad (42)$$

which depends on the mass of the virtual quark-antiquark system  $M_{2|0}^2(x, \vec{q}_\perp) = (\vec{q}_\perp^2 + m^2)/x(1-x)$ . We introduced the longitudinal momentum fraction  $x = q^+/k^+$ . The momentum dependence of the Fermi blocking factors can also be written in terms of  $M_{2|0}$  as

$$f^\pm(M_{2|0}) = \left[ \exp \left\{ \beta \left( \frac{M_{2|0}}{2} \mp \mu \right) \right\} + 1 \right]^{-1}. \quad (43)$$

The thermal mass of the pion  $m_\pi(T, \mu)$  is determined by the pole of  $t_\pi(k)$ .

The integrals involved in (38) and (42) are divergent and need regularisation. We utilise the invariant Lepage-Brodsky (LB) cut-off scheme, which restricts the mass  $M_{2|0}$  by

$$M_{2|0}^2(x, \vec{q}_\perp) = \frac{\vec{q}_\perp^2 + m^2}{x(1-x)} \leq \Lambda_{\text{LB}}^2. \quad (44)$$

We are left with three model parameters, namely the quark current mass  $m_0$ , the coupling constant  $G$ , and the cut-off  $\Lambda_{\text{LB}}$ . These are adjusted such that the pion mass  $m_\pi = 140$  MeV, the pion decay constant  $f_\pi = 93$  MeV, and constituent quark mass  $m = 336$  MeV are obtained correctly. One finds the values

$$\begin{aligned} G &= 5.51 \text{ eV}, \\ m_0 &= 5.67 \text{ MeV}, \\ \Lambda_{\text{LB}} &= 1428 \text{ MeV}. \end{aligned} \quad (45)$$

These correspond to the case I discussed in [39]. Following Ref. [45] the gap equation with LB regularisation in light-front form and the gap equation with 3-momentum (3M) cut-off ( $\vec{k}^2 \leq \Lambda_{3\text{M}}^2$ ) in instant form are equivalent if one chooses a medium dependent LB cut-off

$$\Lambda_{\text{LB}}^2(T, \mu) = 4 (\Lambda_{3\text{M}}^2 + m^2(T, \mu)). \quad (46)$$

The medium dependence of the cut-off may seem artificial at first, but one should notice that the relevant energy scale of the effective field theory changes with the medium parameters.

The in-medium pion mass for different values of the chemical potential is shown in Figure 1.A. The Mott dissociation line is given by the intersection of  $m_\pi(T, \mu)$  and the continuum  $2m(T, \mu)$ . In the NJL model discussed the chiral phase transition occurs

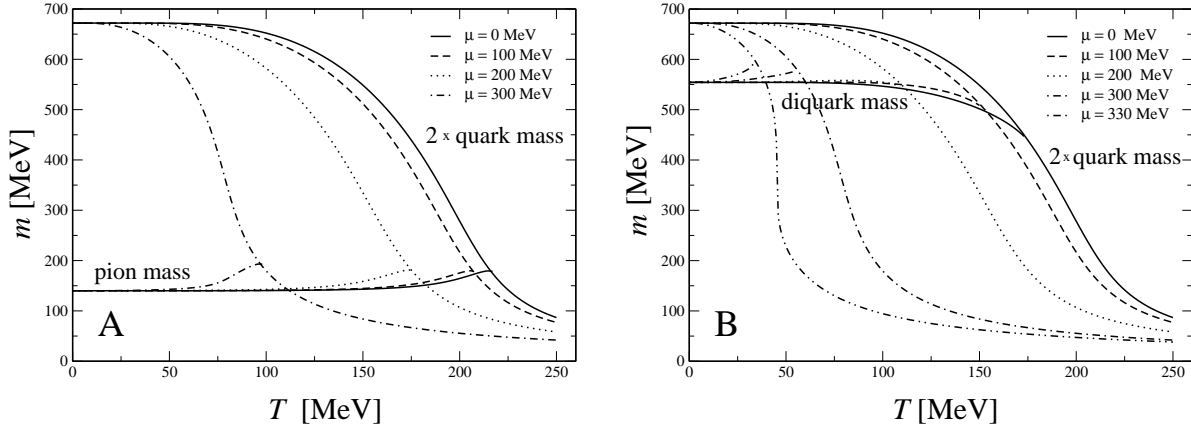


**Figure 1.** (A) The pion mass as a function of  $T$  for different  $\mu$ . (B) The diquark mass as a function of  $T$  for different  $\mu$ . The continuum is given by  $2m$ . The lines of the two-body masses end at the Mott dissociation points.

when  $m(T_c, \mu_c) = m(0, 0)/2$  holds [39]. In Figure 3.B the chiral phase transition ( $T_c, \mu_c$ ) is plotted as solid line and one reads off the critical temperature for vanishing chemical potential as  $T_c = 190$  MeV which is compatible with recent lattice calculations with almost physical quark masses [8]. The dashed line represents the pion dissociation. It worth noting that the pion dissociation and the chiral phase transition line are located in a narrow band of the phase diagram, which is of course expected by Goldstone boson character of the pion. However, both lines do not coincide in this simple model of quark matter, which means that deconfinement and chiral restoration happen at different temperatures and densities in accordance with certain lattice computations [46].

#### 4.2. Diquarks and Colour Superconductivity

The quark-quark interaction is constructed by Fierz transformation of (37), see Reference [47] for details. Let us consider scalar, isospin singlet, colour-antitriplet diquarks, i.e. we choose the following kernel

$$K_{\alpha\beta,\gamma\delta} = 2iG_s(\gamma_5 C \tau_2 \lambda^a)_{\alpha\beta} (C^{-1} \gamma_5 \tau_2 \lambda^a)_{\gamma\delta}, \quad (47)$$

with  $\alpha = 2, 5, 7$  for the anti-symmetric Gell-Mann matrices in standard representation and the charge conjugation matrix  $C = i\gamma^2\gamma^0$ . Analogous to the pion case the reduced  $t$ -matrix  $t_d(k)$  is introduced and the solution

$$t_d(k) = \frac{2iG_d}{1 + 2G_d\Pi_d(k^2)}, \quad (48)$$

contains the diquark loop

$$\Pi_d(k^2) = -3 \int_{\text{LB}} \frac{dx d^2\vec{q}_\perp}{x(1-x)(2\pi)^3} \frac{M_{2|0}^2(x, \vec{q}_\perp) (1 - 2f^+(M_{2|0}))}{M_{2|0}^2(x, \vec{q}_\perp) - k^2}, \quad (49)$$

where the normalisation factor (30) is present.

Results for the medium dependence of the diquark mass  $m_d$  are presented in Figure 1.B. The coupling in the diquark interaction channel is fixed to  $G_d/G_\pi = 1/\sqrt{2}$  which leads to the mass  $m_d \simeq 554$  MeV of an isolated diquark. Interestingly the dependence of the in-medium diquark mass on temperature changes drastically when the chemical potential is increased. While for small  $\mu$  the diquark mass decreases with temperature, the behavior is opposite for  $\mu \gtrsim 200$  MeV. For even larger chemical potentials the chiral phase transition occurs and the diquarks cease to exist as bound states. This turn-around is caused by the competition of two effects, namely Pauli blocking and the in-medium quark mass. The contribution to the diquark loop free from Pauli blockings is still medium dependent and leads to a decreasing bound state mass as the quark mass reduces. Due to the different couplings in the pion and diquark channel one observes this differing behavior of the bound state mass even when the loop integrals (42) and (49) are equal, e.g. for  $\mu = 0$ .

The interaction in the above discussed quark-quark channel is attractive. Therefore one expects the formation of a colour superconducting phase for sufficiently high densities and low temperatures. For two flavours the colour superconducting phase (2SC) is characterised by the condensate  $\Phi = \langle \psi^T C \gamma_5 \tau_2 \lambda_2 \psi \rangle$ , cf. [40] for a review. The  $SU_c(3)$  colour symmetry is broken down to  $SU(2)$ . Usually one derives a gap equation for  $\Phi$  but here we follow a different strategy using the diquark  $t$ -matrix. The Thouless criterion

$$m_d(T, \mu) = 2\mu \quad (50)$$

enables us to compute the boundary to the colour superconducting phase [48]. Equation (50) is a condition for the condensation of bosonic diquarks but remains valid beyond the two quark threshold and leads to the cancelation of the pole present in (49) for  $m_d \geq 2m$ . Inserting (50) into (48) the pole condition becomes

$$\frac{1}{2G_d} = 3 \int_{\text{LB}} \frac{dx}{x(1-x)} \int_{\text{LB}} \frac{d^2 \vec{q}_\perp}{(2\pi)^3} \frac{M_{2|0}^2(x, \vec{q}_\perp) (1 - 2f^+(M_{2|0}))}{M_{2|0}^2(x, \vec{q}_\perp) - 4\mu^2}. \quad (51)$$

Our result is plotted in quark matter phase diagram Figure 3.B. The 2SC phase is located at temperatures below  $T \leq 92$  MeV and for chemical potentials  $300 \text{ MeV} \lesssim \mu \leq 702$  MeV. At  $T = 85$  MeV and  $\mu = 297$  MeV the boundary of the superconducting phase and the chiral phase transition meet. These results are in general agreement with specific scenarios of more sophisticated instant form calculations including various condensates and colour superconducting phases [40].

### 4.3. Nucleon

On the light-front the treatment of the spin is technically involved and for the time being we average over the spin projections. This procedure, used before in Ref. [49] to describe the proton electric form factor with a zero-range interaction, can be justified

in quark matter, because the spins can be regarded as washed out by the medium. Equation (36) evaluated in momentum space for a zero-range interaction reads

$$\Gamma(q) = \frac{2t(P_2)}{(2\pi)^4} \int d^4k R_1^{(0)}(k) N_2(k, P_3 - q - k) R_2^{(0)}(P_3 - q - k) \Gamma(k), \quad (52)$$

where  $R_n^{(0)}$  are  $n$ -body free boson propagators,  $P_3^\mu$  is the three-body energy momentum vector in the center of mass system and the energy momentum vector of the two-body subsystem is given by  $P_2^\mu = P_3^\mu - q^\mu$ . The two-body scattering amplitude  $t(P_2)$  reads

$$t(P_2) = (i\lambda^{-1} - B(P_2))^{-1}, \quad (53)$$

where the loop integral is given by

$$B(P_2) = -\frac{i}{2(2\pi)^3} \int \frac{dx d^2k_\perp}{x(1-x)} \frac{1 - 2f^+(x, \vec{k}_\perp^2)}{P_2^2 - M_{2|0}^2}. \quad (54)$$

One notes the similarity of (49) and (54) but the former integral accounts for the spins of the quarks which then lead to the  $M_{2|0}^2(x, \vec{q}_\perp)$  factor in the numerator. After the integration of (52) the integral equation for the vertex function can be written as

$$\Gamma(y, \vec{q}_\perp) = \frac{i}{(2\pi)^3} t(P_2) \int_0^{1-y} \frac{dx}{x(1-y-x)} \int d^2k_\perp \frac{1 - F(x, y; \vec{k}_\perp, \vec{q}_\perp)}{M_3^2 - M_{3|0}^2} \Gamma(x, \vec{k}_\perp), \quad (55)$$

where the arguments of the blocking factors read

$$F(x, y; \vec{k}_\perp, \vec{q}_\perp) = f(x, \vec{k}_\perp^2) + f(1-x-y, (\vec{k}_\perp + \vec{q}_\perp)^2). \quad (56)$$

The integral involving  $B(P_2)$  has a logarithmic divergence. In order to investigate a solution of the three-body bound state equation, we now extend the LB-regularisation explained in Section 4.1 to the mass of the virtual three-particle state  $M_{3|0}$ , which is the sum of the on-shell minus-components of the three particles, i.e.

$$M_{2|0}^2, M_{3|0}^2 < \Lambda^2. \quad (57)$$

It is not meaningful to use the same value of the cut-off used in the two-body calculations, because the mass of the virtual three-particle state should be  $M_{3|0} \geq 3m$  and in this case we should have a too small integration range. Therefore, we express the parameter in units of the quark mass following [50, 51], i.e.  $\Lambda = \nu m$ . The regularised two-body propagator is then modified as follows

$$B_\Lambda(P_2) = -\frac{i}{2(2\pi)^3} \int_{M_{2|0}^2 \leq \Lambda^2} \frac{dx d^2k_\perp}{x(1-x)} \frac{1 - 2f^+(x, \vec{k}_\perp^2)}{P_2^2 - M_{2|0}^2} \quad (58)$$

and the three-quark equation becomes [50]

$$\Gamma_\Lambda(y, \vec{q}_\perp) = \frac{i}{(2\pi)^3} t_\Lambda(M_2) \int_0^{1-y} \frac{dx}{x(1-y-x)} \int_{M_{3|0}^2 \leq \Lambda^2} d^2k_\perp \frac{1 - f^+(x, \vec{k}_\perp) - f^+(y, (\vec{k}_\perp + \vec{q}_\perp)_\perp)}{M_3^2 - M_{3|0}^2} \Gamma_\Lambda(x, \vec{k}_\perp). \quad (59)$$

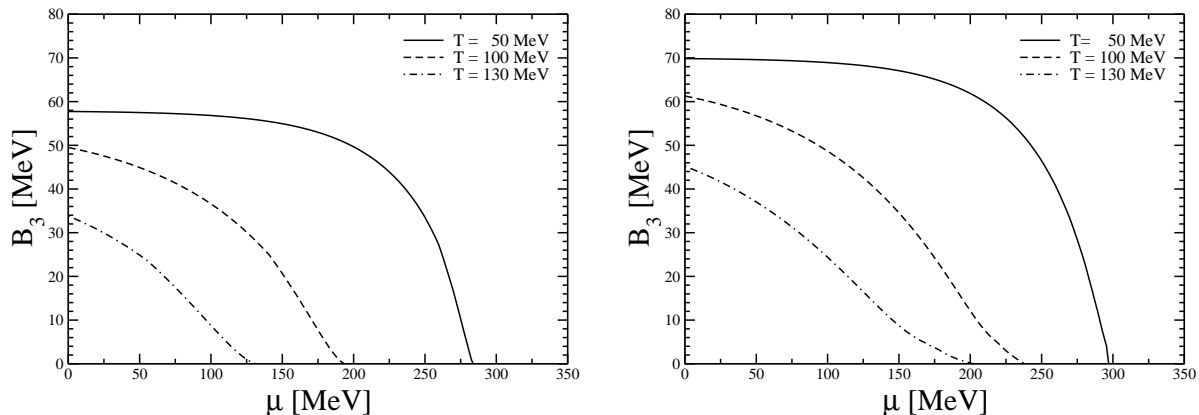


**Figure 2.** Binding energy of the three-quark bound state at various temperatures as indicated for  $\Lambda = 4m$  (left panel) and for  $\Lambda = 10^{15}m$  (right panel)

We have investigated the isolated two- and three-body bound states as a function of the coupling  $\lambda$  for different values of the cut-off parameter and the stability of the three-body problem elsewhere [50, 51]. Choosing  $m = 336$  MeV for the quark mass we constrain our results to the nucleon mass. This determines the function  $\lambda(\Lambda)$  and the model is parameterised by the cut-off  $\Lambda$  only. In the following we use the two limiting cases  $\Lambda = 4m$  and  $\Lambda = 10^{15}m$ .

The solution of (59) allows us to calculate the three-quark binding energy at finite temperatures and the chemical potentials for the different cut-offs defined as

$$B_3(T, \mu) = m(T, \mu) + M_{2B}(T, \mu) - M_{3B}(T, \mu). \quad (60)$$

In Figure 2. the binding energy  $B_3$  as function of the chemical potential for constant values of the temperature using  $\Lambda = 4m$  and  $\Lambda = 10^{15}m$  is shown.  $B_3$  becomes smaller by increasing chemical potential for a constant value of the temperature. We can calculate at which temperature and chemical potential the binding energy vanishes and therefore the three-quark bound states disappear. As before the values of  $T$  and  $\mu$ , for which the nucleon dissociation occurs, define the Mott lines and are shown on the left panel of Figure 3. in comparison with the chiral phase transition. At low temperatures the dependence on the cut-off is mild, but at zero density the different cut-offs  $\Lambda$  give significantly different values for the transition temperature. This can be understood by considering the important role of the colour screening at high density which cancels the details of the dynamics given by the different values of the cut-off. At low densities the effect of the colour screening is negligible and the different dynamics are perceivable. The Mott lines qualitatively follow the chiral phase transition given by the solid line and the nucleon dissociation occurs in the chiral broken phase. An overview of the phase diagram is given on the right side of Figure 3. The interval between these two transitions may be regarded as the confinement-deconfinement region.

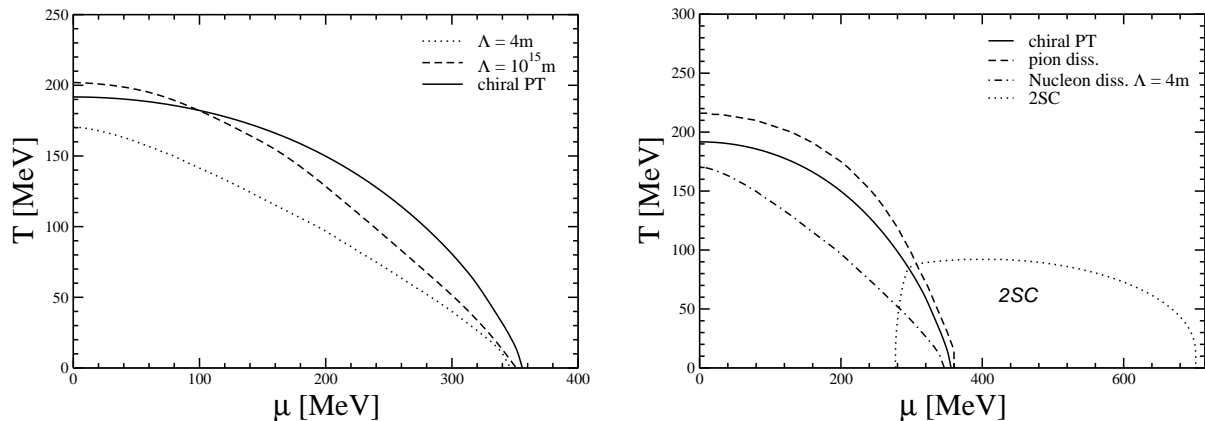


**Figure 3.** (left panel) The Mott lines of the nucleon for  $\Lambda = 4m$  and  $\Lambda = 10^{15}m$ . (right panel) The quark matter phase diagram in the light cone NJL model. The solid line shows the chiral phase transition. The dashed line is the Mott dissociation line of the pion and the dashed-dotted line is the Mott dissociation of the nucleon for  $\Lambda = 4m$ . Finally the transition between the deconfined and the 2SC phase is given by the dotted line.

## 5. Conclusions

Starting from a quasi-particle concept of quarks embedded in a hot and dense medium, we presented a unified description of the most important quark correlations present at the phase transition of QCD. Two challenges have been faced, correlations in a many-particle system and relativity. Correlations within a quasi-particle picture lead, in the simplest case, to (properly modified) few-body equations for two- and three-body states. Relativity leads to kinematical differences and the possibility of pair creation. In addition the strength of the interaction leads to a strong modification of the self energy of the particles. These challenges have been tackled utilising the light-front form of relativity.

The basically Hamiltonian concept of the light-front form allows us to carry the Hamiltonian formulation of nonequilibrium quantum statistics along with the Dyson expansion (or cluster expansion) of many-body Greens functions through to the relativistic regime. For the sake of a unified description we have utilised a simple, but rather useful and hence widely investigated model of QCD, the Nambu–Jona-Lasino model. The basic ingredients of QCD relevant for finite temperature studies are included except for the confinement property. It is reasonable to assume confinement to be screened strong enough due to the presence of the other charged sources in the plasma. In fact, the major quality of this interaction is the zero-range property. Within this context we determine the in-medium properties of pions, diquarks and nucleons and investigated the whole temperature-density plane of the quark matter phase diagram including the chiral phase transition, the onset of the colour superconducting phase and the dissociation lines of pions and nucleons. The later ones give a measure were

the residual interaction between the quarks is weak enough to allow the onset of the confinement-deconfinement phase transition (assuming the colour dependent confining mechanism already screened accordingly).

The physics field that can now be tackled is quite broad ranging from such intriguing questions how hadrons form during the early plasma phase of the universe, whether a colour superconducting phase exists, up to what the nature of QCD phase transition is. In addition, going beyond the quasi-particle approach seems to be straightforward in the Dyson expansion, however, it is still intriguing to arrive at self consistent results. Along this line a next step is the implementation of the full three-body  $t$ -matrix in a computation of the critical temperature of condensation/pairing of diquarks. The present formalism is well suited to address this very interesting problem, hardly investigated in literature.

Besides the Dyson expansion in an equilibrated quasi-particle gas the light-front formulation allows us also to derive relativistic transport equations. First calculations that go beyond the NJL model have already been performed in 1+1 dimensions. Further effort is needed to approach the full 3+1 domain utilising e.g. transverse lattice methods or alike.

## References

- [1] Dirac P A 1949, Rev. Mod. Phys. **21** 392
- [2] S. J. Brodsky, H. C. Pauli and S. S. Pinsky, Phys. Rept. **301**, 299 (1998), and refs. therein.
- [3] K. G. Wilson, Nucl. Phys. Proc. Suppl. **140** (2005) 3 [arXiv:hep-lat/0412043].
- [4] F. Karsch, Nucl. Phys. A **698** (2002) 199 [arXiv:hep-ph/0103314].
- [5] F. Karsch, Lect. Notes Phys. **583** (2002) 209 [arXiv:hep-lat/0106019].
- [6] C. R. Allton, S. Ejiri, S. J. Hands, O. Kaczmarek, F. Karsch, E. Laermann and C. Schmidt, Phys. Rev. D **68** (2003) 014507 [arXiv:hep-lat/0305007].
- [7] C. R. Allton *et al.*, Phys. Rev. D **71** (2005) 054508 [arXiv:hep-lat/0501030].
- [8] M. Cheng *et al.*, Phys. Rev. D **77** (2008) 014511 [arXiv:0710.0354 [hep-lat]].
- [9] M. G. Alford, K. Rajagopal and F. Wilczek, Phys. Lett. B **422** (1998) 247.
- [10] M. G. Alford, K. Rajagopal and F. Wilczek, Nucl. Phys. B **537** (1999) 443.
- [11] R. Rapp, T. Schafer, E. V. Shuryak and M. Velkovsky, Phys. Rev. Lett. **81** (1998) 53.
- [12] K. Rajagopal and F. Wilczek, Shifman, M. (ed.): At the frontier of particle physics, vol. 3\* 2061, hep-ph/0011333.
- [13] M. Gyulassy and L. McLerran, Nucl. Phys. A **750** (2005) 30 [arXiv:nucl-th/0405013].
- [14] P. Jacobs and X. N. Wang, Prog. Part. Nucl. Phys. **54** (2005) 443 [arXiv:hep-ph/0405125].
- [15] H. Stoecker, Nucl. Phys. A **750** (2005) 121 [arXiv:nucl-th/0406018].
- [16] K. Adcox *et al.* [PHENIX Collaboration], Nucl. Phys. A **757** (2005) 184 [arXiv:nucl-ex/0410003].
- [17] E. V. Shuryak, Nucl. Phys. A **750** (2005) 64 [arXiv:hep-ph/0405066].
- [18] U. W. Heinz, AIP Conf. Proc. **739** (2005) 163 [arXiv:nucl-th/0407067].
- [19] H. Song and U. W. Heinz, Phys. Lett. B **658** (2008) 279 [arXiv:0709.0742 [nucl-th]].
- [20] Kadanov L P and Baym G 1962, *Quantum Statistical Mechanics* (Mc Graw-Hill, New York).
- [21] Fetter A L and Walecka J D 1971, *Quantum Theory of Many-Particle Systems* (McGraw-Hill, New York), and Dover reprints 2003.
- [22] Dukelsky J., Röpke G. and Schuck P. (1998), Nucl. Phys. **A 628** 17-40.
- [23] M. Beyer, S. Mattiello, T. Frederico and H. J. Weber, Phys. Lett. B **521** (2001) 33.
- [24] S. Elser and A. C. Kalloniatis, Phys. Lett. B **375** (1996) 285 [arXiv:hep-th/9601045].

- [25] S. Strauss and M. Beyer, Phys. Rev. Lett. **101** (2008) 100402 [arXiv:0805.3147].
- [26] S. J. Brodsky, Fortsch. Phys. **50**, 503 (2002).
- [27] V. S. Alves, A. Das and S. Perez, Phys. Rev. D **66**, 125008 (2002).
- [28] M. Beyer, S. Mattiello, T. Frederico and H. J. Weber, arXiv:hep-ph/0310222.
- [29] S. Dalley and B. van de Sande, Phys. Rev. Lett. **95** (2005) 162001 [arXiv:hep-ph/0409114].
- [30] H. A. Weldon, Phys. Rev. D **67**, 085027 (2003).
- [31] H. A. Weldon, Phys. Rev. D **67**, 128701 (2003).
- [32] A. N. Kvinikhidze and B. Blankleider, hep-th/0305115.
- [33] A. Das and X. x. Zhou, Phys. Rev. D **68**, 065017 (2003).
- [34] J. Raufeisen and S. J. Brodsky, Phys. Rev. D **70** (2004) 085017 [arXiv:hep-th/0408108].
- [35] A. Das, J. Frenkel and S. Perez, arXiv:hep-th/0502243.
- [36] W. Israel, Annals Phys. **100**, 310 (1976).
- [37] W. Israel, Physics **106A**, 204 (1981).
- [38] H. A. Weldon, Phys. Rev. D **26**, 1394 (1982).
- [39] S. P. Klevansky, Rev. Mod. Phys. **64** (1992) 649.
- [40] M. Buballa, Phys. Rept. **407** (2005) 205 [arXiv:hep-ph/0402234].
- [41] M. Beyer, S. Mattiello, T. Frederico and H. J. Weber, J. Phys. G **31** (2005) 21.
- [42] M. Beyer, W. Schadow, C. Kuhrts and G. Ropke, Phys. Rev. C **60** (1999) 034004.
- [43] M. Beyer, S. A. Sofianos, C. Kuhrts, G. Ropke and P. Schuck, Phys. Lett. B **488** (2000) 247
- [44] S. Mattiello, PhD thesis (in german).
- [45] W. Bentz, T. Hama, T. Matsuki and K. Yazaki, Nucl. Phys. A **651** (1999) 143.
- [46] Y. Aoki, Z. Fodor, S. D. Katz and K. K. Szabo, Phys. Lett. B **643** (2006) 46 [arXiv:hep-lat/0609068].
- [47] N. Ishii, W. Bentz and K. Yazaki, Nucl. Phys. A **587** (1995) 617;
- [48] D. J. Thouless, Annals Phys. **10**, 553 (1960).
- [49] W. R. de Araújo, J. P. de Melo and T. Frederico, Phys. Rev. C **52**, 2733 (1995).
- [50] S. Mattiello, Few Body Syst. **34**, 119 (2004).
- [51] Beyer M., Mattiello S., Frederico T. and Weber H.J.: Few Body Syst. **33**, 89 (2003).